Submitted, accepted and published by

Fuel 218 (2018) 417-424

Assessment of Low-cost Oxygen Carrier in South-western Colombia, and its use in the *in-situ* Gasification Chemical Looping Combustion Technology

Francisco J. Velasco-Sarria[a], *Carmen R. Forero*[a*], *Iñaki Adánez-Rubio*[b], *Alberto Abad*[b], *Juan Adánez*[b]

[a] Universidad del Valle, Engineering School of Natural and Environmental Resources (EIDENAR), Calle 13 No. 100-00, 760032057 Cali, Colombia.

[b] Department of Energy and Environment, Instituto de Carboquímica (CSIC), Miguel Luesma Castán 4, 50018, Zaragoza, España.

francisco.velasco@correounivalle.edu.co, carmen.forero@correounivalle.edu.co, iadanez@icb.csic.es, abad@icb.csic.es, jadanez@icb.csic.es

• Corresponding author: Tel: (+57) 3212100 ext 7018. e-mail address: carmen.forero@correounivalle.edu.co (Carmen Rosa Forero). Ciudad Universitaria Meléndez Calle 13 # 100-00. A.A.25360 Cali Colombia.

Submitted, accepted and published by

Fuel 218 (2018) 417-424

Abstract

In Chemical Looping Combustion (CLC), the Oxygen Carrier (OC) is key element of the process. Most OCs have been developed synthetically, using an active metal oxide combined with an inert material. When solid fuels are used, a loss of OC is expected as it mixes with the ashes generated during the CLC process making the costs elevated. As a result, there is a growing interest in using low-cost OCs based in Mn and Fe.

In this research, a by-product derived from manganese ore purification is studied. This material has a high silicon content and it is composed of rhodonite as the main specie and wustite as the minority specie. The material, a Mn mineral from the Nariño department in the Southwest of Colombia, was selected in a previous work based on its good properties such as appropriate crushing strength, an oxygen transport capacity of 3,4 %, and a relatively high reactivity.

Here, tests in a batch fluidized bed reactor were carried out with the selected material with CH_4, CO, and H_2 at 950°C during 50 cycles. A good behaviour was observed with CO and H_2, with a moderate attrition, and lifetime of 2950 hours. The material presented a trend towards agglomerating with CH_4, and no agglomeration with CO and H_2. The possible oxygen uncoupling effect due to the presence of combined oxides of manganese and silicon was also evaluated, but there was no evidence in the 950-1040 ºC interval when the material was oxidized with a 10 vol.% O_2.

Due to its good performance with CO and H_2, the material was evaluated for the *in-situ* Gasification Chemical Looping Combustion (*i*G-CLC) technology, using a Chilean reactive coal as fuel at temperatures from 900 °C to 1000 °C.

Submitted, accepted and published by

Fuel 218 (2018) 417-424

Its good behaviour with H_2 and CO makes it a promising OC for *i*G-CLC technology.

Highlights

- Mn based mineral OXMN010A show good mechanical properties, good reactivity and do not present CLOU properties. Moreover, the lifetime is higher than other natural materials studied so far.
- Due to the good behaviour with CO and H_2, the Mn based waste mineral is considered a suitable to be used in *i*G-CLC.

Keywords: CO_2 capture, coal, low-cost oxygen carriers, *i*G-CLC.

Abbreviations

GHG: greenhouse gases

CLC: Chemical Looping Combustion

IPCC: Intergovernmental Panel on Climate Change

OC: Oxygen-Carrier

OCs: Oxygen-Carriers

*i*G-CLC: *in-situ* Gasification Chemical-Looping Combustion

CLOU: Chemical-Looping with Oxygen Uncoupling

XRF: X-ray fluorescence

XRD, X-ray Diffraction

BET: Brunauer-Emmett-Teller surface area analysis

TGA: Thermogravimetric Analyzer

SCM: Shrinking Core Model

Submitted, accepted and published by

Fuel 218 (2018) 417-424

72 bFB: Batch Fluidized Bed

73 $Me_xO_{y:}$ Óxido metálico

74 ICP: Inductively Coupled Plasma.

Submitted, accepted and published by

Fuel 218 (2018) 417-424

1 Introduction

Nowadays, the increase in greenhouse gas concentration (GHG) is evident. This has led to an increase in global temperature, which in turn as led to climate change [1]. An option to avoid this is through the use of CO_2 capture and storage (CCS).

Chemical Looping Combustion technology (CLC) has emerged as a very attractive option for the capture of carbon dioxide because it inherently separates itself from the other components of the flue gases, i.e. N_2 and O_2 that are not used, so no additional energy is required for their separation [2].

A key element for the development of CLC is the oxygen carrier (OC). When solid fuels are used there are losses of OC because they mix with the ashes of the process. This is the reason why there is a growing interest in low-cost OCs [3]. In this context, the use of minerals in their natural state or industrial waste seems to be very promising because they a have good reactivity with the solid fuel gasification products (H_2 or CO). Low-cost materials are being considered for use with gaseous fuels [4, 5].

Several authors [6, 7] studied Fe-based materials and industrial waste for carbon gasification in situ with CLC (*i*G-CLC), finding that the gasification rate of char decreases when the O/C molar ratio decreases as the concentration of H_2 and CO increases. Bauxite waste (red mud), such as hematite ore was able to burn the gasification products with a high combustion efficiency. These efficiencies are comparable to those obtained under the same conditions using the Fe-based synthetic material.

Fe, Mn oxides are becoming important because they are inexpensive and non-toxic, and their oxygen transport capacity is higher when compared to Fe [8].

The highest oxidation state of Mn is MnO_2 and it decomposes at 500 °C [9]. However, at temperatures above 800 °C only the Mn_3O_4 is present as a stable material [10]. Therefore, only the transformation between Mn_3O_4 and MnO is considered for CLC applications. Mn_2O_3 may be an alternative for the Chemical-Looping with Oxygen Uncoupling process (CLOU), which is based on the decomposition of the metal oxide to Mn_3O_4 and O_2 in reducing atmospheres. Because the CLOU process presents greater efficiencies of CO_2 capture and combustion than the CLC with conventional carriers, it would be extremely interesting to achieve oxidation Mn_2O_3 with air, but the re-oxidation of manganese oxides to Mn_2O_3 is restricted to comparatively low temperatures, around 800 °C, which makes using the CLC technology difficult [11]. The formation of combined oxides can overcome the mechanical and thermodynamic limitations that can present Mn oxides as reported by some authors [5, 11, 12].

Ryden et al [12] provide an overview of the feasibility of developing OCs from combined oxides, that is, oxides with crystalline structures that include several different cations. Since the manganese ions may be present in a large number of oxidation states, the Mn forms oxides with a large number of elements, which may allow the development of OCs from combined oxides that release O_2 in conditions suitable for the CLOU process.

Jing et al [13] studied synthetic combined oxides by mixing Mn_3O_4 and SiO_2 from which manganese silicates are produced, such as: braunite (Mn_7SiO_{12}) and rhodonite

120 ($MnSiO_3$), depending on the SiO_2 content and the calcination temperature. They have
121 found that these species are very important in CLOU behaviour, which was
122 thermodynamically predicted and experimentally tested.
123 Also, they observed a total conversion with syngas (50% CO – 50% H_2) for the
124 materials with low content of SiO_2 and the attrition rate of the tested oxygen carriers
125 was very high and varied from 3,9 wt%/h to 40,2 wt% /h.

126 With respect to natural minerals, different lifetimes have been reported in literature
127 for Fe ore (1600 h) [14], Ilmenite (700 h) [15] and Mn ore (284 h) [16] when used in
128 CLC due to their attrition during CLC . Mei et al [17] studied different Mn minerals in
129 *i*G-CLC with bituminous coal as the fuel finding instantaneous char gasification rates
130 higher than Ilmenite and iron ore.

131 In a previous study [18] of 8 Fe and Mn minerals found in Colombia, a screening of
132 different materials was made and its reaction kinetics was studied using
133 thermogravimetric analysis, a Mn mineral, from the Nariño department in the
134 Southwest of Colombia was selected (OXMN010A) due to its good properties.
135 The main component identified in this mineral is rhodonite ($MnSiO_3$) with one small
136 fraction of wustite (FeO). Reduction and oxidation reactions for this mineral are
137 shown in *Table 1* [12].

138

139

140

Submitted, accepted and published by

Fuel 218 (2018) 417-424

Table 1. Reduction-oxidation Reaction for OXMN010A

Sample	Reactive	Reactions
OXMN010A	CH_4	$2Mn_7SiO_{12} + 12SiO_2 + \frac{3}{2}CH_4 \rightarrow 14MnSiO_3 + \frac{3}{2}CO_2 + 3H_2O$
	CO	$Mn_7SiO_{12} + 6SiO_2 + 3CO \rightarrow 7MnSiO_3 + 3CO_2$
	H_2	$Mn_7SiO_{12} + 6SiO_2 + 3H_2 \rightarrow 7MnSiO_3 + 3H_2O$
	O_2	$14MnSiO_3 + 3O_2 \rightarrow 2Mn_7SiO_{12} + 12SiO_2$

The objective of this work is to study the behaviour of a mineral of Mn (OXMN010A) in a batch fluidized bed (bFB) with gaseous (CLC) and solid (iG-CLC) fuels to know its suitability as oxygen carrier material.

2 Experimentation

2.1 Oxygen carrier

The OXMN010A material, from the department of Nariño-Colombia, was selected through a previous study [18]. Sampling is performed according to the ASTM D2234 norm [19]. The characterization is performed by: crushing strength analysis, surface area analysis (BET), X-ray fluorescence analysis (XRF) and X-ray diffraction (XRD) using Thermo Scientific equipment, model ARL9900 Workstation with an X-ray tube for fluorescence with rhodium anode. In *Table 2* the results obtained for the mineral's characterization are shown.

OXMN010A is subjected to a thermal treatment (heating at 1050 °C for 4 hours with air at atmospheric pressure) and the crushing strength is measured before and after

158 this in order to verify its improvement with the thermal treatment. A crushing strength
159 greater than 1 N is considered acceptable [20] within the screening processes that
160 allow the selection of an OC with the appropriate mechanical properties. The result of
161 the crushing strength after the heat treatment is 3 N, which is equivalent to a 29%
162 increase. This result is in agreement with that reported by some authors [13, 21].

163 Table 2. Characterisation of OXMN010A mineral used in tests for Chemical
164 Looping Combustion (CLC) and *in-situ* Gasification Chemical-Looping Combustion
165 (*i*G-CLC)

Particle diameter (µm)	Oxygen transport capacity (% w/w)	Crushing strength (N)	Surface Area BET (m^2/g)	Elementary composition (XRF) [a]							Crystalline phases (XRD) [b]	
				Si	Al	Fe	Ca	Mg	Ti	Mn	MnSiO3 (Rodonite)	FeO (Wüstite)
100-300	3,4	2,3	23,3	13	2,5	3,5	1,9	0,8	0,2	35,7	85,4	6,1

166 [a] Percent in % w/w. Values less than 0,1 are negligible.
167 [b] Percent in % w/w.
168

169 In the bFB experiment with coal, a subbituminous coal from Mina Invierno in Riesco
170 Island (Chile) was used. The proximate and ultimate analyses are shown in *Table 3*.

171 Table 3. Proximate and ultimate coal analysis used for tests in *i*G-CLC

Analysis	Dry basis	Wet basis
Moisture (% w/w)		15,2
Ash (% w/w)	17,9	15,1
Volatile matter (% w/w)	39,3	33,4
Fixed carbon (% w/w)	42,8	36,3
Carbon (% w/w)	61,1	51,8
Hydrogen (% w/w)	4,3	3,6
Nitrogen (% w/w)	0,9	0,8
Sulfur (% w/w)	0,2	0,2
Oxygen (% w/w)[a]	15,7	13,3

172 [a] Determined by difference

Submitted, accepted and published by

Fuel 218 (2018) 417-424

2.2 Experimental facilities

The realization of several reduction-oxidation cycles in a batch fluidized bed reactor (bFB) are an approximation to the continuous conditions the OC will be subjected to. To evaluate the precision of the experiments in CLC, 50 redox cycles were carried out at each condition and two test were carried out in some cases in iG-CLC. This allows one to know the distribution of gaseous products, the agglomeration of the material, the attrition of the solid and the carbon deposition. For the study of the behaviour of OXMN010A with gaseous and solid fuels, the setup presented in *Figure 1* was used. This is located at the Instituto de Carboquímica (CSIC) Zaragoza. The reactor is made of Kanthal, its internal diameter is 0,054 m and its height is 0,5 m, with a preheating zone of 0,3 m just below the distributor plate. The experimental setup contained a solid fuel feeding system to feed batches of coal to the bottom part of the fluidized bed.

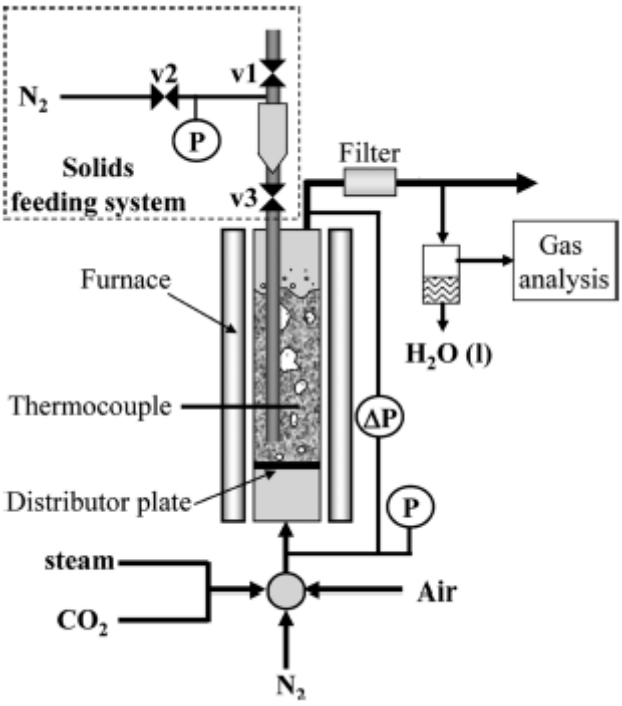

Figure 1. Batch Fluidized Bed (bFB) diagram used in Chemical Looping Combustion (CLC) and *in-situ* Gasification Chemical-Looping Combustion (*i*G-CLC) tests.

2.2.1 Chemical looping combustion (CLC)

To characterise the performance of the oxygen carrier 50 redox cycles were carried out in the bFB. The reduction time was 60 s and the oxidation time was 360 s for CO, 480 s for H_2 and 600 s for CH_4 and the purge time was 180 s. A sample of 150 g of OC, a gas flow rate of 230 LN/h at a fluidization velocity of 0,12 m/s (u/umf > 2.1). The working conditions that are presented in *Table 4* were selected in order to maintain the same oxygen consumption and to make comparisons between the fuel gases. O_2 at 10 % was selected as the oxidizing gas, simulating the mean oxygen concentration in an air reactor (AR). Furthermore, the temperature in the bed is controlled during the oxidation this way, as there is no cooling system. The gas composition at the outlet of the bFB reactor is measured continuously with different gas analysers. Concentrations of CO, CO_2 and CH_4 were measured in a non-dispersive infrared analyser (NDIR) (Siemens ULTRAMAT 23), the concentration of H_2 is determined by a thermal conductivity detector (Maihak S710/THERMOR) and the concentration of O_2 was determined with the use of a paramagnetic analyser (Siemens OXYMAT 5E).

Table 4. Experimental design for chemical looping combustion (CLC) tests

Fuel	%	N_2 to balance	Oxidant	%	N_2 to balance
CH_4	25	75	O_2	10	90
CO-CO_2	50-20	30	O_2	10	90
H_2	50	50	O_2	10	90

A sample is taken at the end of the 50 operating cycles to characterise the oxidized and/or reduced species.

2.2.2 *In-situ* gasification chemical-looping combustion (*i*G-CLC)

During the evaluation of the behaviour of the mineral OXMN010A in the *i*G-CLC technology, the experiments were carried out using a gas flow of 172 L_N/h and various carbon masses (0,5 g 1,0 g 1,5 g 2,0 g and 2,5 g) at temperatures of 900 °C, 950 °C and 1000 °C. The tests were carried out with 150 g of OC. Blank tests are carried out using 150 g of sand. Water vapour and/or N_2 was used as a gasifying agent and a fluidizing medium in the reduction stage. When the carbon is introduced it is fluidised with N_2. In N_2, the char was converted very little because the solid-solid interaction between the char and the OC is very slow [22]. After the pyrolysis is completed, water vapour and N_2 were allowed to pass. During the reduction period, the coal was fed into the bed and was gasified. The gasification products (CO and H_2) react with the oxygen carrier particles to yield CO_2 y H_2O. After a purge period with nitrogen (3 minutes), the OC in the bed is regenerated using a current of 10% of O_2 and N_2 to balance. During the reduction and oxidation, the reactor's outlet gas streams were analysed after condensing water. Concentrations of the dry gases (CO, CO_2, CH_4, H_2 and O_2) were determined using the analysers previously described.

2.3 Data processing

2.3.1 With gaseous fuels (CH_4, CO, H_2) (CLC)

To evaluate the behaviour of the OXMN010A material, the following analyses were performed on the fresh and used materials from the bFB experimentation: crushing

strength, AJI attrition index [23], particle distribution, SEM and ICP. To determine the attrition, a pair of heated filters were used at the outlet of the reactor, which are monitored periodically, to determine the loss of fine particles from the bed. The attrition rate, A (%/h), is defined in the Equation (1), where p_f is the weight of the elutriated particles < 45 μm during a Δt, p_t is the total weight of the solid inventory and ∆t is the period of time, in seconds, during which the particles are collected [24, 25].

$$A = \frac{p_f}{p_t * \Delta t} * 3600 * 100 \quad (1)$$

Attrition can be used to estimate the half-life of the particles as 100/A.

Taking the final attrition value measured and 8640 h of annual operation of the CLC plant, the required solid inventory must be completely replenished n_r times per year according to Equation (2).

$$n_r = \frac{8640 * A}{100} \quad (2)$$

The agglomeration was detected when the pressure drop decreases in respect to that corresponding to the fluidization of 150 g of bed, as described by Cho et al. [26]. Further to that, at the end of the cycles the presence of agglomeration in the bed is visually observed.

The particle diameter distribution is performed on a Beckman Coulter LS 13 320 device with the laser diffraction method which measure the particle size distribution from the angular variation of scattered light intensity when a lightning Laser passes through a sample of dispersed particles. The particle size was recorded as a sphere diameter in accordance with the volume. In the tests carried out a sweep of particle

diameters between 0,375 um and 2000 um was carried out with which the amount of material at 10%, 25%, 50%, 75% and 90% was determined and the distribution graph of the particle diameter as a function of volume was created.

Based on the distribution of gases from the outlet stream in the reduction stage, the balance of atoms for the oxygen is performed, where the rate of oxygen transferred from the OC to the gaseous fuel, $r_{O,r}(t)$, is determined using Equation (3) and the conversion of the solid, X_{OC}, is calculated using Equation (4) and Equation (5). Finally, the conversions of the solid in the bFB are compared during the reduction for the different fuels and the total conversion of the fuel (X_{fuel}).

$$r_{O,r}(t) = (y_{CO} + 2y_{CO_2} + y_{H_2O})_s F_s \quad (3)$$

$$X_{OC}(t) = \frac{1}{N_{O,OC}} \int_{t_{r,0}}^{t} r_{o,r}(t)dt \quad (4)$$

$$N_{O,OC} = \frac{m_{ox} R_{O,OC}}{M_O} \quad (5)$$

Where y_i is the concentration of compound *i* at the reactor's outlet, F_s is the molar flow of the outlet gas stream of the bFB, $N_{O,OC}$ are the moles of oxygen in the OC available for the reaction and M_O Is the molar mass of oxygen. The fuel conversion is calculated using Equation (7), where r_{fuel} is the flow of fuel leaving the unreacted bFB and N_{fuel} is the fuel that enters the bFB.

$$r_{fuel}(t) = (y_{fuel})_s F_s \quad (6)$$

$$X_{fuel}(t) = 1 - \frac{\int_{t_{r,0}}^{t} r_{fuel}(t)dt}{N_{fuel}} \quad (7)$$

The oxygen conversion rate in the oxidation stage, $r_{O,o}(t)$, can be calculated in an analogous way, taking into account the formation of CO and CO_2 during this period

due to the oxidation of possibly existing C from the decomposition of fuel in the reduction period. In this case the amount of oxygen transferred from the air to the OC, $r_{O,o}$ is calculated using Equation (8) where F_e Is the molar flow of the inlet gas stream of the bFB and y_i is the molar fraction of the gas *i*.

$$r_{O,o}(t) = (y_{O_2})_e F_e - \left(y_{O_2} - 0{,}5y_{CO} - y_{CO_2}\right)_s F_s \quad (8)$$

The rate index is quantified, in order to determine the reactivity of the material and to make comparisons with Mn minerals reported in the literature. This parameter is calculated using the equation (9) and equation (10). To determine the rate index, the experimental data found for cycles 10, 30 and 50 are used with the different fuel gases (CO, H_2 and CH_4).

$$rate\ index = 100 * 60 * Roc * \left(\frac{dX_i}{dt}\right)_{norm} \quad (9)$$

$$\left(\frac{dX_i}{dt}\right)_{norm} = \frac{P_{ref}}{P_{TGA}} * \frac{dXi}{dt} \quad (10)$$

where*:* Roc Is the oxygen transport capacity of the material,$\frac{\mathrm{dX_i}}{\mathrm{dt}}$ is the derivative of the conversion of component *i* in relation to the time, P_{ref} is the reference pressure (0,15 atm) of the fuel gas and P_{TGA} is the partial fuel pressure for bFB experiments.

2.3.2 In-situ gasification chemical-looping combustion (*i*G-CLC)

In this work, the effect of the selected oxygen carrier at the gasification stage, as well as its efficiency in the conversion of the gasification products to CO_2 and H_2O, is evaluated. Starting from a carbon balance, the conversion rate of char $r_C(t)$, is determined using Equation (11), where F_S is the dry basis gas flow calculated from

285 the N_2 introduced into the reactor F_{N_2} to maintain enough gas flow into the gas
286 analysers and y_i is the molar fraction of component *i* (CO_2, CO and H_2) at the outlet
287 of the reactor.
288

$$r_c(t) = \left(y_{CO_2} + y_{CO}\right)F_s \quad (11)$$

$$F_s = \frac{F_{N_2}}{1 - \sum_i y_i} \quad (12)$$

289 Using the conversion rate of the char (Equation (11)) one can determine the
290 conversion of char, X_{char} (Equation (13)), where $N_{C,char}$ are the carbon moles in the
291 fixed carbon of the coal. The instant conversion rate of char $r_{C,inst}(t)$ (Equation (14
292)) is defined as the rate of gasification in reference to the amount of non-gasified
293 carbon in the reactor.

$$X_{char}(t) = \frac{\int_0^t r_c(t)dt}{N_{C,char}} \quad (13)$$

$$r_{C,inst}(t) = \frac{r_C(t)}{N_{C,char}(1 - X_{char})} \quad (14)$$

294 The oxygen transfer rate from the OC to the solid fuel, $r_O(t)$, is determined using
295 Equation (15) and it is integrated to calculate the conversion of the oxygen carrier,
296 $X_{OC,iG-CLC}$, using Equation (16) at any moment in time. The combustion efficiency of
297 the char is determined using Equation (17)

$$r_O(t) = F_s(2y_{CO_2} + y_{CO} - y_{H_2}) \quad (15)$$

$$X_{OC,iG-CLC}(t) = \frac{1}{N_{O,OC}} \int_0^t r_O(t)dt \quad (16)$$

$$\eta c(t) = \frac{r_O(t)}{2\, r_{C,inst}(t)} \quad (17)$$

3 Results and discussion

Table 2 represents the characterisation of sample OXMN010A. The result of the XRF analysis shows the presence of Mn and Si in high concentration. When mixed, these oxides form combined oxides that have a good oxygen transport capacity ($R_{O,OC}$) and may have a CLOU effect [12]. According to the crushing strength analysis (2,3 N) the mineral meets one of the requirements to be considered as a material with high mechanical resistance [20]. It also has a high surface area (23,3 m^2/g) indicating a greater area of contact between OC and the working gases, a condition that favours the CLC process. These surface area results are much higher than those reported in the literature about manganese ores (0,6 m^2/g a 7,1 m^2/g) [27]. The semi-quantitative results of the XRD analysis show the presence of rhodonite ($MnSiO_3$) as the main specie and wustite (FeO) as the minority specie, which has been cited in the literature as OCs [12, 13, 21].

Previous studies have shown the chemical reactions of reduction and oxidation for the OXMN010A, which are presented in *Table 1*. In addition, mineral OXMN010A has been found to have good reactivity and stability with the number of cycles [18].

3.1 Experiments in batch fluidized bed reactor with gaseous fuels (CLC)

Since Jing et al [13] evidenced the CLOU effect when working with synthetically manufactured braunite (Mn_7SiO_{12}) and rhodonite ($MnSiO_3$), in this study experiments

were carried out with N_2 as the reducing gas and 10% O_2 as the oxidizing gas at temperatures of 950 ^{o}C, 1000 ^{o}C and 1040 °C, observing that the OXMN010A does not present any CLOU effect, which is in contradiction with that indicated in the study of Jing et al, which may be attributed to the presence of other minority species present in the natural mineral.

For the experiment in CLC with gaseous fuels, the product distribution is determined from the recorded data of the gas concentration at the outlet of the reactor at each time interval and the conversion of the OC is quantified as a function of time. *Figure 2* shows the evolution of the concentration of gases in a redox cycle with CH_4, H_2 and CO. In the case of CH_4 in the reduction stage, it can be seen how there is no complete conversion since part of the CH_4 is found to be unreacted. The presence of CO_2 once the oxidation is initiated can be seen in *Figure 2.* This indicates the carbon deposition during reduction with CH_4. In the case of H_2 the conversion to H_2O is complete and for CO a fraction close to 5% remains unreacted.

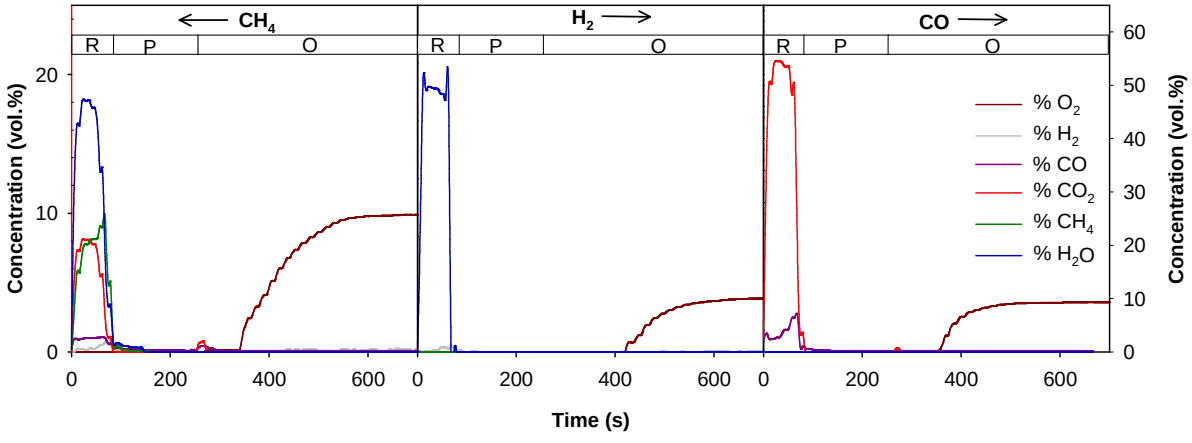

Figure 2. Product distribution vs. time during reduction (R), purging (P) and oxidation (O) in CLC tests for OXMN010A with gaseous fuels at 950 °C. Reduction: 25% CH_4, 50% H_2 or 50% CO, Oxidation: 10% O_2. Balance: N_2. Cycle 10

335

336 The distribution of gaseous products obtained during the reduction period determines
337 the amount of oxygen transferred from the OC (X_{OC}) toward the fuel gas, using
338 Equation (4). The results of X_{OC} for the selected OC (OXMN010A) are presented in
339 *Figure 3* and show a higher conversion with CO (19,6 %) and H_2 (20,1 %) than with
340 CH_4 (15,1%), in 60 seconds.

341 The uncertainty associated with the dispersion of data (type B) with a reliability of
342 95% is 0,7%, 0,5% and 0,1%, respectively. These results are in line with what was
343 found in the previous kinetic study performed by the authors [18] . The behaviour in
344 cycles 10, 30 and 50 can also be observed (*Figure 3*) and a similar behaviour is
345 presented which guarantees the stability of the OXMN010A with the number of
346 cycles. Although there is a small decrease in CO conversion in the final cycles. The
347 conversion efficiencies of the fuels are calculated using Equation (7), they are: CH_4
348 63%, for H_2 99 % and for CO 92 %. This indicates that the OXMN010A is not suitable
349 for use as oxygen carrier with natural gas, but its use for iG-CLC can be proposed.

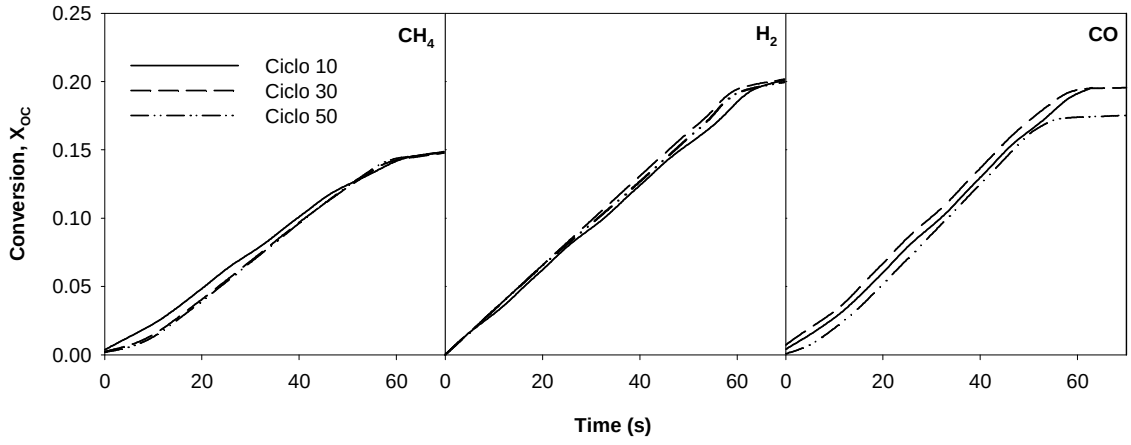

350
351 Figure 3. Oxygen carrier conversion, $X_{OC,}$ vs. time during several cycles of reduction
352 in CLC tests for OXMN010A at 950 °C with gaseous fuels. Reduction: 25% CH_4, 50%
353 H_2 or 50% CO, Oxidation: 10% O_2.

354

355 The rate index is an important parameter that allows comparisons of the reactivity of
356 the OCs. The quantification of the rate index values for mineral OXMN010A with CO,
357 H_2 and CH_4 are calculated using Equation (9) and are presented in *Table* 5. For
358 OXMN10A it can be seen how this parameter is greater for CO and H_2 than for CH_4
359 therefore this mineral is more reactive with the main products of the gasification (CO
360 and H_2) than with CH_4.

361 The rate index calculated in the present work suggests that the reactivity of the
362 OXMN010A, comparing with the available data in the literature for Mn minerals, was
363 equal to the maximum value with CH_4, was slightly lower than the reported minimum
364 with H_2 and was higher than that reported for CO.

365 Table 5. Rate index for CH_4, CO and H_2 for different OCs in bFB at 950 ^oC

Oxygen Carrier	Fuel	Rate Index in bFB (%/min)
OXMN010A	CH_4	0,6
	CO	1,4
	H_2	1,3
Mn Mineral [28]	CH_4	0,4 - 0,6
	CO	0,4 - 1,0
	H_2	1,5 - 2,0
Activated Ilmenite [29]	CH_4	0,4 - 0,5 [a]
	CO	0,3 - 0,4 [a]
	H_2	1,2 - 1,5 [a]

366 [a] Rate index at 950 °C of activated ilmenite estimated from Cuadrat et al. [29]

367 According to Abad et al.[30] a 50% increment of reduction rate for activated ilmenite
368 was attained by changing the temperature from 900 to 950 °C. Thus in order to
369 compare the reactivity of OXMN010A with ilmenite, this 50% increment was used,

because ilmenite was work at 900 ^{o}C. The rate index calculated for OXMN010A suggests that the reactivity was similar to or even higher than that found for ilmenite with CH_4, was higher than that of ilmenite with CO and similar with H_2.

Given the good behaviour of this mineral with the main gasification products (H_2 and CO) and since the presence of the CLOU effect is not evident because there is no release of O_2, the OXMN010A presents a great potential use with solid fuels for *i*G-CLC.

3.2 Experiments in batch fluidized bed reactor with coal (*i*G-CLC)

The performance tests of the OXMN010A in *i*G-CLC were carried out with feeding of batches of 0,5 g, 1,0 g, 1,5 g, 2,0 g and 2,5 g of sub-bituminous coal. During the reduction stage of the tests, 2 peaks will be presented in the reading of the outlet gas stream of the bFB (*Figure 4*). The first one corresponds to the pyrolysis and combustion of the volatiles and the second one to the gasification of the char. The ore evaluation as an oxygen carrier has focused on the second stage, because the gasification controls the overall mechanism of the reaction due to being the slowest stage. It is assumed that fixed carbon is equivalent to the char and as the volatiles are removed in the initial stage. This corresponds entirely to carbon (42,8 % dry basis, *Table 3*).

Submitted, accepted and published by

Fuel 218 (2018) 417-424

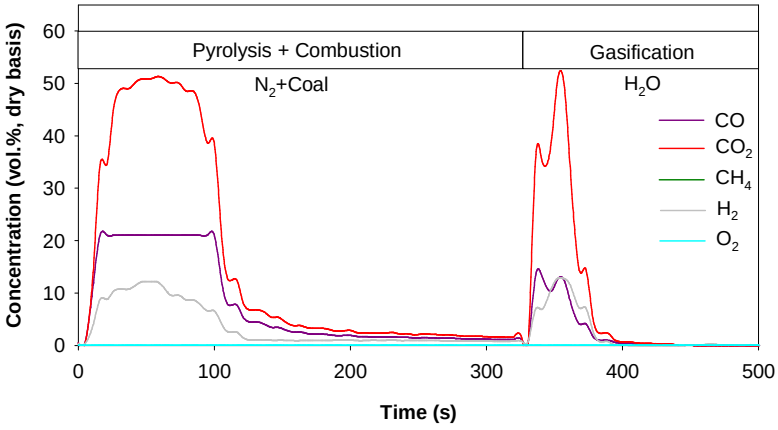

Figure 4. Product distribution vs. time during pyrolysis + combustion and gasification in *i*G-CLC test for OXMN010A at 950 °C with coal. Fuel: 2,5 g of subbituminous coal. Oxidation: 10% O_2. Balance: N_2.

Since the OXMN010A shows a good reactivity with CO and H_2, as the results show in CLC tests, a low production of CO and H_2 is expected. *Figure 4* shows a large production of CO_2 due to the combustion reaction of the OC with the products of the gasification H_2 and CO, although a part of these remains unreacted in the reduction stage. This same behaviour was found in the tests performed at 900 °C, 950 °C and 1000 °C.

Although not shown in *Figure 4*, it is worth clarifying that after the purge, the OXMN010A is quickly regenerated with a stream of O_2 at 10 % in N_2 to balance. In the oxidation stage there is no production of CO and CO_2, therefore, a complete oxidation of the char ($X_{char} = 1$) occurs in the previous stage of reduction.

3.2.1 Evaluation of the char conversion (X_{char}) and the carrier ($X_{OC,iG-CLC}$)

For comparison purposes the blank tests with sand were used to compare the behaviour with OXMN010A during the reduction with CO and H_2 generated during

409 the coal gasification stage. In *Figure 5*, the char conversion, X_{char} (Equation (13)),
410 the oxygen carrier conversion, $X_{OC,iG-CLC}$ (Equation (16)) and the product
411 distribution (vol. %) as a function of the time of the gasification step are shown. The
412 carbon balance is closed with an approximate error rate of 5%. The effect of a blank
413 test against the mineral OXMN010A is compared in the reduction at 950 °C. When
414 the coal reacts in the presence of the sand (*Figure 5*, Sand), the main products are
415 H_2 and CO, which are the main products of gasification. The oxygen carrier
416 conversion is zero, because there is no oxygen carrier and at 80 s the char
417 conversion is 1,0, because all the carbon is converted to CO and CO_2.
418 When the oxygen carrier reacts with coal (*Figure 5*, OXMN010A), the main product is
419 CO_2, because the C of the char react with the lattice O of the OXMN010A through
420 reaction with the gasification products. An oxygen carrier conversion of 0,44 was
421 found, which corresponds only to the oxygen transferred in the gasification stage
422 because part of the oxygen contained in the carrier is used in the combustion of the
423 products of the previous stage of pyrolysis. The behaviour is the same at 900 °C and
424 1000 °C, finding an oxygen carrier conversion between 0,44 and 0,48.
425

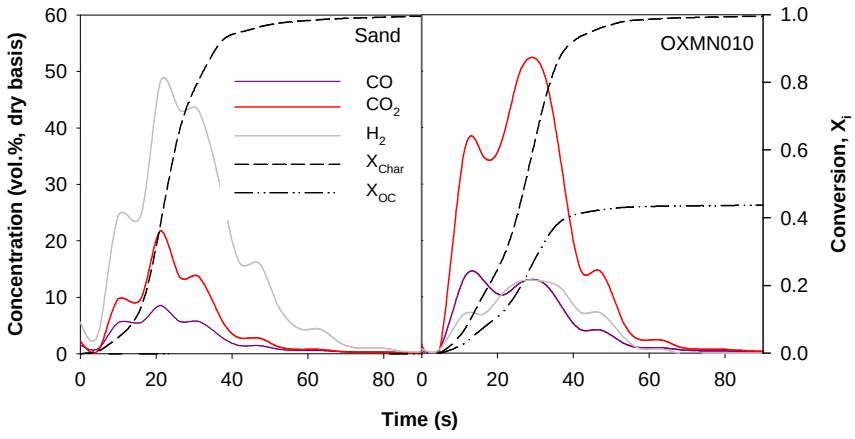

426

Figure 5. Product distribution and conversion (X_i: X_{char} or X_{OC}) vs. time during the char gasification at 950 °C happening in the reduction stage, being either sand or OXMN010A the bed material. Fuel: 2,5 g of subbituminous coal. Oxidation: 10% O_2. Balance: N_2.

A char conversion of 1,0 have been found at 80 s too. This shows how the char is gasified and reacts with the carrier to mainly yield CO_2 and H_2O, in addition to achieving a complete conversion. Mei et al [17] have found the char conversion rate is higher in the presence of the oxygen carrier when compared to a sand bed, which is different with the results of this study, in which the conversion rate are the same in both cases. Maybe this is due to the direct use of coal, which gives highly a reactive char that more reactive than char previously produced.

3.2.2 Influence of temperature and char conversion on the instantaneous rate of gasification ($r_{C,inst}$).

In order to evaluate the behaviour of OXMN010A during the char gasification stage, experiments at three temperatures were performed in the bFB. *Figure 6* (A) shows the behaviour of instantaneous gasification rate of versus char conversion for OXMN010A with subbituminous coal at 900 °C, 950 °C and 1000 °C.

The increase of the instantaneous rate with the increase of char conversion at all temperatures can clearly be seen, however at 950 °C a maximum instantaneous rate is observed at a conversion of 0,65, which corresponds to a reaction model of porous solids taking into account pore growing [28]. Also it shows how the instantaneous rate and the reactivity increases with the temperature. The instantaneous rate increases with the temperature and this increase is near three times in the working

452 range. The instantaneous rate values found are higher than those reported for iron
453 ore [6] .

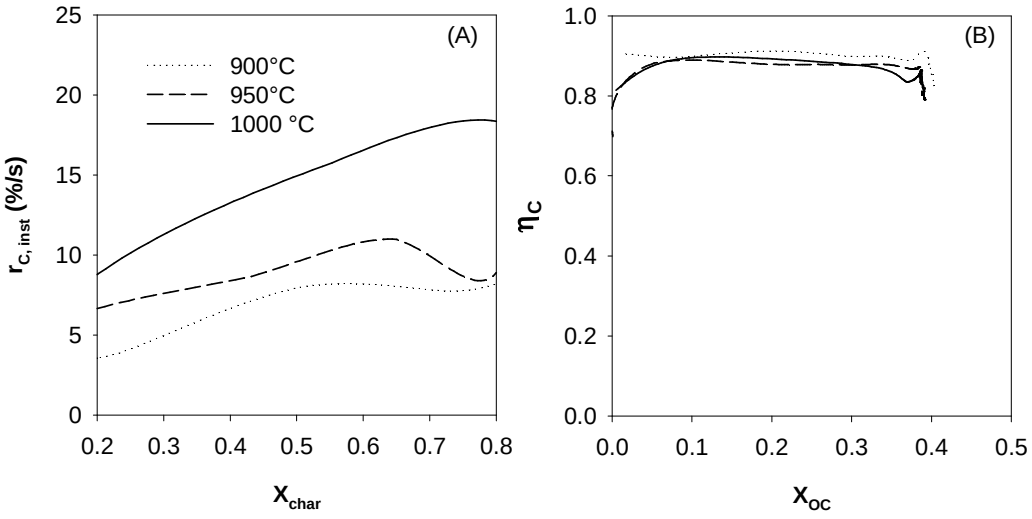

454

455

456 *Figure 6. (A)* Conversion rate of char ($r_{C,inst}$) vs. conversion of char (X_{char}) and (B)
457 Combustion efficiency (η_C) vs. oxygen carrier conversion (X_{oc}) during reduction *i*G-
458 CLC tests for OXMN010A at 900 °C, 950 °C and 1000 °C. Fuel: 2,5 g of
459 subbituminous coal. Oxidation: 10% O_2.

460 Figure *6* (B) shows the combustion efficiency (η_C) vs. oxygen carrier conversion (X_{OC})
461 for OXMN010A with subbituminous coal at different temperatures. High combustion
462 efficiencies higher than 0,85 amongst 900 °C and 1000 °C are found during
463 conversion, At the end of the experiment η_C decreases due to decrease in the
464 availability of oxygen in the carrier. It is also evident how the combustion efficiency is
465 very similar for the three temperatures. The combustion efficiency corresponds to the
466 conversion of the gasification products, which is high.

467

3.2.3 Fluidization behaviour

The OXMN010A did not present agglomeration in the tests carried out with coal, CO and H_2, although with CH_4 they form small agglomerates that are undone when touched with the fingers.

The attrition of OC was also studied during CLC redox cycles with fuel gases. This study has not been performed in the iG-CLC tests, because it is difficult to distinguish the oxygen carrier from the ashes. *Figure 7* shows the attrition rate behaviour (%/h) over time for the OXMN010A. A similar attrition behaviour with the three fuels employed (CH_4, H_2, CO) can be clearly seen. At the beginning is high and decreases with the time. After 14 hours the attrition rate is the same for all fuels with an average value of 0,03 %/h. It should be noted that this estimate is valid only for the time in which the experiment was performed, although it seems to continue decreasing. Taking this value of 0,03 %/h, a lifetime of ~2950 hours of the OC particles for each fuel used was calculated, which is higher than those reported in literature for Fe ore (1600 h) [14], Ilmenite (700 h) [15] and Mn ore (284 h) [16]. To extrapolate this value to a large-scale CLC unit, it is necessary an oxygen carrier makeup to renew the solid inventory three times per year. This is a normal process renewal rate. These results are considered acceptable, as a particle lifetime superior to 2000 h is adequate. This is equivalent to a number of annual replacements of OC between 3 and 4.

Submitted, accepted and published by

Fuel 218 (2018) 417-424

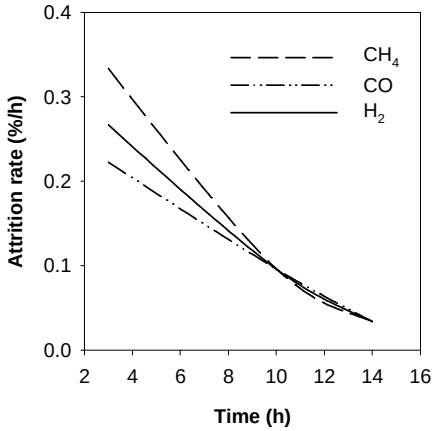

Figure 7. Attrition rate values (%/h) of OXMN010A obtained during CLC tests for OXMN010A with different gaseous fuels at 950 °C. Reduction: 25% CH_4, 50% H_2 or 50% CO, Oxidation: 10% O_2.

To analyse the effect of the combustion with gases on the particles of the OXMN010A, the particle size distribution analysis is performed on fresh and used particles after 50 redox cycles.

The results of the particle distribution in (*Figure 8*) for the samples used with respect to the fresh samples of the mineral OXMN010A show a small decrease in the particle distribution. It is seen that there is a fraction of large particles that do not undergo change. Intermediates are those that decrease in size, and smaller ones also decrease in size but less so, which is not a pattern of fragmentation, but attrition by wear (friction). In addition, there is no variation in the original shape of the samples nor agglomeration.

Submitted, accepted and published by

Fuel 218 (2018) 417-424

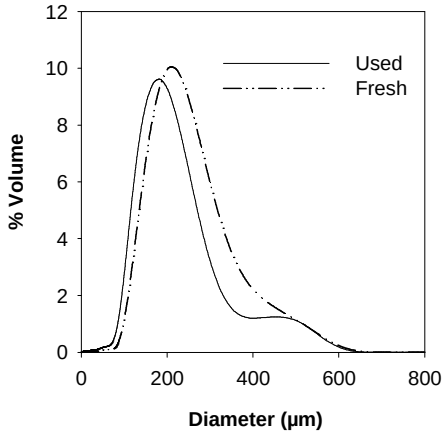

Figure 8. Particle diameter distribution for fresh and used samples in CLC tests for OXMN010A at 950 °C. Reduction: 50% H_2 and 50% N_2. Oxidation: 10% O_2.

Although the experimentations were performed only in bFB, the methodology proposed by Cabello et al [20] could be used as a screening tool to evaluate the mechanical behaviour of mineral OXMN010A. Table 6 shows the AJI index values, which are below 5%, which is a value considered acceptable for FCC (Fluid Catalytic Cracking) catalysts. The AJI index for used particles is similar to the value for fresh particles indicating that the effect of the redox cycles on the particle integrity is small. Also, the crushing strength is higher than 1 N, therefore the material should not be discarded for its mechanical behaviour for continuous scaling in CLC.

ICP analysis is performed on the fresh and used samples to determine Fe, Mn and Si concentration. These results are fully consistent with the XRF analyses performed on all initial materials reported in *Table 2*. The presence of Mn and Si in significant concentrations is also evident, although the used particles present an enrichment in Fe and loss of Mn, that merits a future analysis.

Table 6. Characterization of fresh and used samples in chemical looping combustion (CLC) test for OXMN010A at 950 °C. Reduction: 50% H_2 and 50% N_2. Oxidation: 10% O_2 and N_2 to balance.

Parameter	Fresh	Used
AJI (%)	4,1	4,3
Crushing Strength (N)	3,0	2,0
Fe (% w/w)[a]	2,4	3,4
Mn (% w/w)[a]	38,4	36,9
Si (% w/w)[a]	15,8	17,0

[a] Determined by ICP

The OXMN010A has proven to be very reactive, both with gases and with coal, has a rate index comparable to other minerals and a longer lifetime than other natural materials studied so far. In addition, it is important to highlight these results taking into account that the OXMN010A is a residue of manganese mining.

4 Conclusions

A mineral waste (OXMN010A) has been characterized for CLC demonstrating its suitability for *i*G-CLC. Although this mineral ore shows the presence of rhodonite ($MnSiO_3$) as the main reduced specie, it does not present the CLOU effect.

Since the mineral shows good reactivity especially with CO and H_2, it exhibits a great potential to be used in iG-CLC, which has been demonstrated during the experiment with a reactive sub-bituminous coal. Its reactivity is higher than in other minerals used in this technology.

The mineral exhibits good mechanical and fluidization properties, the average lifetimes of the particles are greater than 2000 h, the AJI index for the sample used is less than 5 and the crushing strength is greater than 1 N. This indicates that it meets

the necessary mechanical requirements according to the methodology proposed in the literature [20]. The lifetime of OXMN010A is higher than other natural materials studied so far.

Acknowledgements

This research was conducted with financial support from the Unión Temporal Incombustion (Temporary Joint Working Group) and Colciencias through the Contract of Contingent Recovery RC 0852-2012 and to the collaboration of Instituto de Carboquímica (CSIC) from Zaragoza. Thanks to Ing. Konrad Holscher from Mina Invierno (Chile) for supplying the subbituminous coal batch.

5 BIBLIOGRAFIA

1. IPCC, *Climate Change 2014 Synthesis Report, Fifth Assessment Synthesis Report*. 2014, United Nations Organizations.

2. IPCC, *Special report on carbon dioxide capture and storage*. 2005, Cambridge University Press, Cambridge, United Kingdom and New York, NY, USA: Prepared by Working Group III of the Intergovernmental Panel on Climate Change [Metz, B., O. Davidson, H. C. de Coninck, M. Loos, and L. A. Meyer (eds.)].

3. Zhao, H.B., H.G. Jin, and R.X. Cai, *Theory study on the performance of compressor-stepless-cooling gas turbine.* Kung Cheng Je Wu Li Hsueh Pao/Journal of Engineering Thermophysics, 2001. **22**(4): p. 408.

4. Leion, H., T. Mattisson, and A. Lyngfelt, *Use of ores and industrial products as oxygen carriers in chemical-looping combustion*. Energy and Fuels, 2009. **23**(4): p. 2307-2315.

5. Fossdal, A., et al., *Study of inexpensive oxygen carriers for chemical looping combustion.* International Journal of Greenhouse Gas Control, 2011. **5**(3): p. 483-488.

6. Mendiara, T., et al., *Low-cost Fe-based oxygen carrier materials for the iG-CLC process with coal. 1*. Industrial and Engineering Chemistry Research, 2012. **51**(50): p. 16216-16229.

7. Abad, A., et al., *Low-cost Fe-based oxygen carrier materials for the iG-CLC process with coal. 2*. Industrial and Engineering Chemistry Research, 2012. **51**(50): p. 16230-16241.

8. Velasco-Sarria, F., C. Forero, and E. Arango, *Low-cost oxygen carriers in chemical looping combustion (CLC) and its potencial in Colombia.* Dyna Energía y Sostenibilidad, 2017. **6**(1): p. 21.

9. Stobbe, E.R., B.A. de Boer, and J.W. Geus, *The reduction and oxidation behaviour of manganese oxides.* Catalysis Today, 1999. **47**(1-4): p. 161-167.

10. Zafar, Q., et al., *Reduction and oxidation kinetics of Mn3O4/Mg-ZrO2 oxygen carrier particles for chemical-looping combustion.* Chemical Engineering Science, 2007. **62**(23): p. 6556-6567.

11. Mattisson, T., A. Lyngfelt, and H. Leion, *Chemical-looping with oxygen uncoupling for combustion of solid fuels.* International Journal of Greenhouse Gas Control, 2009. **3**(1): p. 11-19.

12. Rydén, M., et al., *Combined oxides as oxygen-carrier material for chemical-looping with oxygen uncoupling.* Applied Energy, 2014. **113**: p. 1924-1932.

13. Jing, D., et al., *Examination of oxygen uncoupling behaviour and reactivity towards methane for manganese silicate oxygen carriers in chemical-looping combustion.* International Journal of Greenhouse Gas Control, 2014. **29**: p. 70-81.

14. Adanez, J., et al., *Progress in chemical-looping combustion and reforming technologies.* Progress in Energy and Combustion Science, 2012. **38**(2): p. 215-282.

15. Lyngfelt, A. and B. Leckner, *A 1000MWth boiler for chemical-looping combustion of solid fuels – Discussion of design and costs.* Applied Energy, 2015. **157**: p. 475-487.

16. Schmitz, M., et al., *Chemical-Looping Combustion of Solid Fuels Using Manganese Ores as Oxygen Carriers.* Energy & Fuels, 2016. **30**(2): p. 1204-1216.

17. Mei, D.F., et al., *Manganese Minerals as Oxygen Carriers for Chemical Looping Combustion of Coal.* Industrial & Engineering Chemistry Research, 2016. **55**(22): p. 6539-6546.

18. Velasco-Sarria, F., et al., *Reduction and oxidation kinetics of Fe-Mn based minerals of sourthweestern Colombia for Chemical Looping Combustion.* In process selection, 2017.

19. ASTM, *D2234/D2234M-10 Standard Practice for Collection of a Gross Sample Of Coal*. 2010: Philadelphia United State.

20. Cabello, A., et al., *On the attrition evaluation of oxygen carriers in Chemical Looping Combustion.* Fuel Processing Technology, 2016. **148**: p. 188-197.

21. Frick, V., et al., *Screening of supported and unsupported Mn–Si oxygen carriers for CLOU (chemical-looping with oxygen uncoupling).* Energy, 2015. **93, Part 1**: p. 544-554.

22. Mendiara, T., et al., *Evaluation of the use of different coals in Chemical Looping Combustion using a bauxite waste as oxygen carrier*. Fuel, 2013. **106**: p. 814-826.

23. ASTM, *D5757-11 Standard Test Method for Determination of Attrition of FCC Catalysts by Air Jet Stand*. 2011: Philadelphia United State.

24. Cabello, A., et al., *Long-lasting Cu-based oxygen carrier material for industrial scale in Chemical Looping Combustion.* International Journal of Greenhouse Gas Control, 2016. **52**: p. 120-129.

25. Forero, C., *Combustión de gas con captura de CO2 mediante transportadores sólidos de oxigeno a base de CuO*, in *Departamento de Ingeniería Química y Tecnologías del Medio ambiente* 2011, Zaragoza: Zaragoza.

26. Cho, P., T. Mattisson, and A. Lyngfelt, *Defluidization conditions for a fluidized bed of iron oxide-, nickel oxide-, and manganese oxide-containing oxygen carriers for chemical-looping combustion.* Industrial and Engineering Chemistry Research, 2006. **45**(3): p. 968-977.

27. Arjmand, M., et al., *Investigation of different manganese ores as oxygen carriers in chemical-looping combustion (CLC) for solid fuels.* Applied Energy, 2014. **113**(0): p. 1883-1894.

28. Mei, D., et al., *Evaluation of Manganese Minerals for Chemical Looping Combustion.* Energy and Fuels, 2015. **29**(10): p. 6605-6615.

29. Cuadrat, A., et al., *Behavior of ilmenite as oxygen carrier in chemical-looping combustion.* Fuel Processing Technology, 2012. **94**(1): p. 101-112.

30. Abad, A., et al., *Kinetics of redox reactions of ilmenite for chemical-looping combustion.* Chemical Engineering Science, 2011. **66**(4): p. 689-702.